Title

Enhancer additivity and non-additivity are determined by enhancer strength in the Drosophila embryo

Journal

eLife, 4(AUGUST2015)

Authors

Bothma, JP
Garcia, HG
Ng, S
et al.

Publication Date

2015-08-12

DOI

10.7554/eLife.07956.001

Peer reviewed

Enhancer additivity and non-additivity are determined by enhancer strength in the Drosophila embryo

Jacques P. Bothma[*,1], Hernan G. Garcia[*,2,4], Samuel Ng[1], Michael W. Perry[1,5], Thomas Gregor[#,2,3], and Michael Levine[#,1,6,7]

Affiliations

[1]Department of Molecular and Cell Biology, University of California, Berkeley, CA 94720, USA

[2]Department of Physics, Princeton University, Princeton, NJ 08544, USA

[3]Lewis-Sigler Institute for Integrative Genomics, Princeton University, Princeton, NJ 08544, USA

Current Address

[4]Department of Molecular and Cell Biology, Department of Physics, and Biophysics Graduate Group, University of California, Berkeley, CA 94720, USA

[5]Department of Biology, New York University, 100 Washington Square East, New York, NY 10003, USA

[6]Lewis-Sigler Institute for Integrative Genomics, Princeton University, Princeton, NJ 08544, USA

[7]Department of Molecular Biology, Princeton University, Princeton, NJ 08544, USA

*These authors contributed equally to this work

[#]Corresponding authors. tg2@princeton.edu; msl2@princeton.edu

Abstract

Metazoan genes are embedded in a rich milieu of regulatory information that often includes multiple enhancers possessing overlapping activities. Here we employ quantitative live imaging methods to assess the function of pairs of primary and shadow enhancers in the regulation of key patterning genes—***knirps***, ***hunchback,*** and ***snail***—in developing ***Drosophila*** embryos. The knirps enhancers exhibit additive, sometimes even super-additive activities, consistent with classical gene fusion studies. In contrast, the ***hunchback*** enhancers function sub-additively in anterior regions containing saturating levels of the Bicoid activator, but function additively in regions where there are diminishing levels of the Bicoid gradient. Strikingly sub-additive behavior is also observed for ***snail***, whereby removal of the proximal enhancer causes a significant increase in gene expression. Quantitative modeling of enhancer-promoter interactions suggests that weakly active enhancers function additively while strong enhancers behave sub-additively due to competition with the target promoter.

Introduction

There is emerging evidence that metazoan genes occur in a complex regulatory landscape encompassing numerous enhancers[1–8]. For example, the mouse *Sonic Hedgehog* gene is regulated by at least 20 different enhancers scattered over a distance of ~1 Mb[1]. Individual enhancers mediate expression in a variety of different tissues, including the brain, floorplate, and limb buds. Multiple enhancers with overlapping regulatory activities are also used to control gene expression within individual cell types. For example, the transcriptional activation of the gap gene *hunchback (hb)* in the early *Drosophila* embryo is mediated by both a proximal enhancer and distal "shadow" enhancer that independently mediate activation in response to high levels of the Bicoid activator gradient[7]. Despite overwhelming evidence of multiple enhancers mediating activity of the same gene it is completely unknown how several enhancers interact simultaneously with the same promoter in a given cell. Here we use a combination of quantitative live imaging and theoretical modeling to investigate the function of multiple enhancers for the regulation of a common target gene within a single cell type.

The fate map of the adult fly is established by ~1,000 enhancers that regulate several hundred patterning genes during the one-hour interval between two and three hours after fertilization[9,10]. As many as half of these genes contain "shadow" enhancers with overlapping spatiotemporal activities that are thought to improve the precision and reliability of gene expression[3–6,11,12]. For example, the

hb shadow enhancer helps produce a sharp boundary of activation by the Bicoid gradient, while its *snail* counterpart helps ensure reliable activation under stressful conditions such as high temperatures[3,11]. There is emerging evidence that shadow enhancers are used pervasively in a variety of developmental processes, in both invertebrates and vertebrates[5,12–14].

The underlying mechanisms by which two enhancers with extensively overlapping regulatory activities produce coordinated patterns of gene expression are uncertain. It is possible that they augment the levels of gene expression above the minimal thresholds required to execute appropriate cellular processes[15,16]. However, there is currently only limited experimental evidence for enhancers acting in an additive fashion[13,14]. An alternative view is that shadow enhancers suppress transcriptional noise and help foster uniform expression among the different cells of a population[7]. To explore these and other potential mechanisms we examined the timing and levels of gene activity using BAC transgenes containing individual enhancers and combinations of primary and shadow enhancers in the early *Drosophila* embryo.

BAC transgenes containing three key patterning genes, *hb*, *knirps (kni)*, and *snail (sna)*, were examined in living precellular embryos. Quantitative analyses suggest that shadow enhancers mediate different mechanisms of transcriptional activity. For *kni* we observe additive, even super-additive, activities of the primary and shadow enhancer pairs. In contrast, the *hb* enhancers function sub-additively

in anterior regions containing saturating levels of the Bicoid activator, but function additively in regions where there are diminishing levels of the Bicoid gradient. Strikingly sub-additive behavior is also observed for sna, in that removal of the proximal enhancer causes a significant increase in gene expression. These observations suggest that the levels of enhancer activity determines the switch between additive and non-additive behaviors.

Using theoretical modeling we suggest that these behaviors can be understood in the context of enhancers competing or cooperating for access to the promoter. Weak enhancers work additively due to infrequent interactions with the target promoter, whereas strong enhancers are more likely to impede one another due to frequent associations. Our results highlight the potential of combining quantitative live imaging and modeling in order to dissect the molecular mechanisms responsible for the precision of gene control in development[15], and provide a preview into the complex function of multiple enhancers interacting with the same promoter.

Results

Previous live-imaging studies have relied on simple gene fusions containing a single enhancer attached to a reporter gene with MS2 stem loops inserted in either the 5' or 3' UTR[16–18]. Detection depends on the binding of a maternal mRNA-binding fusion protein (MCP::GFP) expressed throughout the early embryo. In order to examine the interplay between multiple enhancers we created a series of BAC transgenes containing complete regulatory landscapes (summarized in Fig. 1). The BAC transgenes contain an MS2-yellow reporter gene in place of the endogenous transcription units (Fig. 1A). For each locus, *hb*, *kni*, and *sna*, we examined a series of three BAC transgenes: containing both primary and shadow enhancers, as well as derivatives lacking individual enhancers (Fig. 1B,C). As expected, the BAC transgenes containing both enhancers produce robust expression of the MS2 reporter gene that recapitulate endogenous patterns previously measured using mRNA FISH and immunostaining[3,11] (Fig. 1, D-I, Movie 1-3).

Enhancer "deletions" were created by substituting native sequences with neutral sequences of similar sizes (see Methods). These substitutions remove most of the critical sequences identified by ChIP-Seq assays[3,10,19]. It is nonetheless possible that critical flanking sequences persist within the transgenes. However, removal of both *kni* enhancers eliminates detectable transcripts in abdominal regions of early embryos (Fig. S1), suggesting that any remaining flanking sequences are insufficient to mediate expression.

Qualitative inspection of the *hb* and *kni* expression movies suggests that removal of either the primary or shadow enhancer does not cause a dramatic alteration in the overall patterns of gene activity. In order to identify more nuanced changes we quantified the transcriptional activities of the complete series of BAC transgenes (Fig. 2). The fluorescence intensities of active transcription foci were measured during nuclear cleavage cycles (nc) 13 and 14 at different positions across the anterior-posterior (AP) axis. These intensities were converted into an absolute number of elongating Pol II molecules by calibrating with internal standards (see ref. 18). Several embryos were analyzed for each time-point, and the data were merged to determine the average behavior as a function of AP position and time.

Hb expression was examined during the ~15 min interphase of nc 13 when both the primary and shadow enhancers are active, but before the onset of later-acting "stripe" enhancers during nc 14[3,20]. We measured the transcriptional activity of all three *hb* BAC transgenes (Fig. 1D,F,H). Contrary to simple expectations suggested by previous studies[13] we find that the two *hb* enhancers do not function in an additive fashion in anterior regions (20 – 40 % egg length, EL) of the embryo (e.g., Fig. 2A,B). Indeed, the levels produced by the wild-type transgene fall far short of the additive levels predicted by simply summing the levels of expression produced by the transgenes containing either the shadow or primary enhancer alone (Fig. 2A,B). Moreover, the removal of the shadow

enhancer has no effect on the levels of transcription in anterior regions, which is consistent with the original conception of the shadow enhancer as a “back-up” in the event of stress[6].

A very different scenario is observed in central regions of the embryo (40–50 % EL) where *hb* expression switches from “on” to “off” to form a sharp border[21]. In this region the wild-type transgene produces significantly higher levels of expression than either of the transgenes driven by a single enhancer. In fact, these levels correspond to the values predicted by simply adding the activities of the single-enhancer transgenes. Thus, the two enhancers transition from *sub-additive* to *additive* behavior in the region of the embryo where there are diminishing levels of the Bicoid activator gradient. We therefore suggest that the *hb* enhancers function additively only when they are operating below peak capacity (see below).

To further explore the activities of multiple enhancers we examined the *kni* gene, which is regulated by an intronic enhancer and a distal 5’ enhancer[3]. We focus our analysis on central regions of the abdominal expression pattern since previous studies suggest the occurrence of long-range repressive interactions that establish the borders of the “stripe”[3]. During early periods of nc 14 the two enhancers function super-additively (Fig. 2C). That is, the wild-type *kni* BAC transgene produces higher levels of expression than the predicted sum of the two transgenes containing either enhancer alone. During later stages of

development there is a 2-fold reduction in the expression levels of the endogenous gene, and at this time the two enhancers work in a simple additive manner (Fig. 2D). Note that the maximum number of elongating polymerase (Pol II) complexes falls short of that seen for *hb* (compare with Fig. 2A,B).

Understanding the stark difference in the behaviors of the *hb* and *kni* enhancer pairs necessitates measuring the absolute strengths of the different enhancers. Using absolute counts of mRNA molecules[22], we calibrated our live fluorescence intensity traces to determine the average numbers of actively elongating Pol II transcription complexes[17]. The *kni* transgenes containing single enhancers exhibit as little as 4-fold lower levels of expression as compared with the corresponding *hb* transgenes (Fig. 3A,B). At peak activity the proximal *hb* enhancer induces ~50 transcribing Pol II complexes across the yellow reporter gene. By contrast, individual *kni* enhancers produce an average of only ~15 elongating Pol II complexes. We propose that the additive and super-additive behaviors of the two *kni* enhancers reflect their inherently “weaker” activities as compared with the “stronger” proximal hb enhancer (see Discussion). Note that despite these differences, the overall output of transcripts and the overall rate of transcript production are essentially identical for all gap genes[22].

To test the proposed anti-correlation between enhancer strength and additivity we analyzed the expression of *sna*, which is essential for delineating the invaginating mesoderm during gastrulation. *sna* transgenes containing either the

proximal or distal enhancer produce peak transcriptional activities of ~40 actively transcribing Pol II complexes across the *yellow* reporter gene, similar to the numbers seen for the proximal *hb* enhancer (Fig. 3C). Thus, both *snail* enhancers are strong and they exhibit striking sub-additive behaviors. In particular, the wild-type transgene displays significantly lower levels of expression than the mutant transgene containing only the shadow enhancer. Thus, strong enhancers not only fail to function additively, but interfere with one another, leading to sub-additive expression levels. This observation is also consistent with an earlier study, which suggested that the weaker proximal enhancer attenuates the activities of the stronger distal shadow enhancer[21].

In an effort to understand how multiple enhancers might function additively or sub-additively, we developed a mathematical model for dynamic enhancer-promoter interactions. In this model a single enhancer interacts with its promoter via a forward rate k_{on} and a backward rate k_{off} (Fig 4A). The relative values of the forward and reverse rates determine the strength of the enhancer-promoter interaction by controlling what fraction of time the two are bound. When the enhancer and promoter interact the promoter is in the ON state and initiates transcription at a rate r. This rate can be interpreted as the efficiency of enhancer-mediated transcriptional initiation upon enhancer-promoter interaction. Hence the observable rate of mRNA production depends on the interaction strength given by the ratio k_{on}/k_{off}, and the efficiency r with which transcription is initiated upon interaction (Fig. 4B). This scheme can be generalized to include

two enhancers (A and B) interacting with the same promoter (Fig. 4C and see Materials & Methods for details of the mathematical analysis).

When the individual enhancers interact infrequently with the promoter ($k_{on}/k_{off}<<1$) they are unlikely to engage the promoter simultaneously. In this regime the enhancers will work additively, and the rate of mRNA production of enhancers A and B will simply be the sum of the production rate of A and B alone as shown in Fig 4D. However, as the strength of promoter-enhancer interactions increases, the combined activity of both enhancers is less than the sum of each individual enhancer. When we model enhancers of different strengths (Fig. 4E), the amount of mRNA production is reduced as the enhancer with the weaker transcriptional efficiency interacts more frequently with the promoter. This occurs because the two enhancers compete for access to the promoter, effectively inhibiting one another. Thus, weak enhancers might work additively due to infrequent interactions with the target promoter, whereas strong enhancers interfere with one another due to more frequent interactions (see below).

Discussion

Our quantitative analysis of *hb* and *kni* expression provides seemingly opposing results. For *kni* we observe additive, sometimes even super-additive, action of the two enhancers within the presumptive abdomen. In contrast, the two *hb* enhancers do not function in an additive fashion in anterior regions, but are additive only in central regions where expression abruptly switches from “on” to “off”. We propose that “weak” enhancers function additively or even super-additively, whereas “strong” enhancers can impede one another (Fig. 5).

Additional support for this view is provided by the analysis of *sna*. We found that the removal of the proximal enhancer significantly augments expression, consistent with the occurrence of enhancer interference within the native locus. It is also conceivable that a single strong enhancer (e.g., *hb* proximal or *sna* distal) already mediates maximum binding and release of Pol II at the promoter, and additional enhancers are therefore unable to increase the levels of expression. However, the increase in the levels of *sna* expression upon removal of the primary enhancer is inconsistent with this explanation. Perhaps the proximity of the proximal enhancer to the *sna* promoter gives it a “topological advantage” in blocking access of the distal enhancer[23]. The proximal enhancer might mediate less efficient transcription than the distal enhancer, and thereby reduce the overall levels of expression (see Fig. 4E). We do not believe that this proposed difference is due to differential rates of Pol II elongation since published[17] and preliminary studies suggest that different enhancers and promoters lead to

similar elongation rates (~2 kb/min; T. Fuyaka and M. Levine, unpublished results). A nonexclusive alternative possibility is that deletion of the proximal enhancer removes associated *sna* repression elements[24], thereby augmenting the efficiency of the distal enhancer.

A minimal model of enhancer-promoter associations provides insights into potential mechanisms. In the parameter regime where such interactions are infrequent the two enhancers display additive behavior. However, in the regime of frequent interactions, enhancers compete for access to the promoter resulting in sub-additive behavior. Enhancer-promoter interaction parameters are likely to vary not only between different enhancers, but also as the input patterns are modulated in time and space during development[25,26].

This simple model explains the switch from sub-additive to additive enhancer activities for *hb* and *sna*. However, in order to explain the super-additive behavior of the *kni* enhancers, it would be necessary to incorporate an additional state in the model, whereby both enhancers form an active complex with the same target promoter. Such a complex would have a more potent ability to initiate transcription than individual enhancer-promoter interactions.

In summary, we propose that enhancers operating at reduced activities (“weak enhancers”) can function in an additive manner due to relatively infrequent interactions with their target promoters. In contrast, “strong” enhancers might

function sub-additively due to competition for the promoter (Fig. 4E). For *hb* this switch between competitive and additive behavior occurs as the levels of Bicoid activator diminish in central regions where the posterior border of the anterior Hb domain is formed. Similarly, stress might reduce the performance of the *sna* enhancers to foster additive behavior under unfavorable conditions such as increases in temperature[11]. Our study highlights the complexity of multiple enhancers in the regulation of gene expression. They need not function in a simple additive manner, and consequently, their value may be revealed only when their activities are compromised.

Material and Methods

Cloning and Recombineering

In brief, BAC clones that map to the region of interest were identified from end-sequenced BAC libraries which can be viewed on a browser at http://pacmanfly.org, and ordered from BacPac Resources (http://bacpac.chori.org/)[27]. These BACs arrive already cloned into a vector containing attB sequence for targeted integration, mini-white cassette, chloramphenicol resistance, and are in the inducible copy number strain EPI300 (Epicentre Biotechnologies). The following CHORI BACs were used as a starting point: sna BAC (CH322-18I14-1), hb BAC (BAC CH322-55J23), kni BAC (CH322-21P08).

BACs requiring modification were first transformed into the recombineering strain SW102, which was obtained from NCI-Frederick Biological Resources Branch. Cultures containing specific BACs were grown overnight and recombination functions were induced as described[11]. The induced bacteria were electroporated with targeting constructs that were prepared previously by PCR amplification. Targeting constructs were made using a pair of 90 base pair long oligonucleotides. These contained 25 base pairs specific to the region being amplified that was to be swapped into the BAC, and an additional 65 base pairs of sequence homologous to the target BAC flanking the region to be replaced. The homologous regions, or “homology arms”, target the amplified sequence to the region of interest for recombination. After electroporation and a one hour

recovery period in 2XYT broth, bacteria were plated in a dilution series on LB plates with the appropriate antibiotic for overnight incubation at 30C. Individual resulting colonies were screened by PCR for appropriate recombination at both homology arm locations. Confirmed positive recombinant colonies were transformed back into EPI300 cells (Epicentre Biotechnologies) and reconfirmed by antibiotic marker selection and PCR; PCR products were sequenced for final confirmation.

Oligonucleotides for amplification to make homology arm constructs (90 base pairs in length) were from Integrated DNA Technologies (IDT); shorter primers for colony screening PCR were from ELIM Biopharmaceuticals. Restriction enzymes were from New England Biopharmaceuticals. Qiagen products were used to isolate plasmid DNAs, gel-purify DNA fragments, and purify PCR products. Qiagen taq polymerase was used in colony PCR screening; Invitrogen Platinum pfx was used to amplify targeting constructs.

The first step in the modification was to replace the endogenous coding sequence of snail, hb and kni genes with that of the yellow-kanamycin reporter gene. The yellow-kanamycin fragment was swapped into the place of the endogenous gene at the ATG start codon at the 5’ end, leaving the 5’ UTR intact. The endogenous 3’ UTR was also left fully intact. In most cases the different enhancers were replaced with an ampicillin resistance cassette which was PCR amplified from pBluescript. In the case of kni one of the enhancers is in the intron

of the transcribed region and so we replaced enhancer with a fragment of lambda phage DNA using galK positive and negative selection. The next step required the insertion the MS2 stem loop sequences. Copies of the MS2 stem loops were extracted from plasmid pCR4-24XMS2SL-stable (Addgene 31865) and were PCR amplified with primers with appropriate homology sequences.

BAC Preparation for Microinjection and phiC31-Mediated Integration

BACs were induced to high copy number using Epicentre BAC autoinduction solution, according to supplier's instructions, and grown overnight for 16-18 hours at 37C. DNA was prepared for micro-injection using the Invitrogen PureLink HiPure miniprep kit by following manufacturer instructions with described modifications for BACs and cosmids. DNA was diluted to a final concentration of ~300-400 ng/uL and 1x injection buffer. At least 200 embryos were injected per construct by BestGene Inc. (Chino Hills, CA). The transgenes were integrated into the following landing sites: BDSC 9723, BDSC 9750 and BDSC 24749. *Hb* lacking shadow and *kni* lacking primary were integrated into 9750 and 24749, respectively, while all other transgenes were integrated into 9723.

Live imaging sample preparation and data acquisition

Female virgins of line yw; Histone-RFP;MCP-NoNLS-GFP[17] were crossed with males of each reporter line. Collected embryos were dechorinated using bleach and mounted between a semipermeable membrane (Biofolie, In Vitro Systems & Services) and a coverslip (1.5, 18 mm x 18 mm) and embedded in Halocarbon

127 oil (Sigma). The flattening of the embryos makes it possible to image a larger number of nuclei in the same focal plane without causing significant changes in early development processes [28].

Embryos were either imaged using a custom-built two-photon microscope[29] and a Zeiss LSM 780 confocal microscope. Imaging conditions on the two-photon microscope were as described in Garcia et al. 2013. The average laser power at the specimen was 10 mW, the pixel size was set to 220 nm and a single image consisted of 512 x 256 pixels. At each time point a stack of 10 images separated by 1 µm was acquired resulting in a final time resolution of 37s. Confocal imaging was performed using a Plan-Apochromat 40x/1.4NA oil immersion objective. The MCP-GFP and Histone-RFP were excited with a laser wavelength of 488 nm and 561 nm, respectively. Fluorescence was detected with two separate photomultiplier tubes using the Zeiss QUASAR detection unit (gallium-arsenide-phosphide photomultiplier was used for the GFP signal while the conventional detector was used for the RFP). Pixel size is 198 nm and images were captured at 512x512 pixel resolution with the pinhole set to a diameter of 116 µm. At each time point a stack of 22 images separated by 0.5 µm were captured, spanning the nuclear layer. The final time resolution is 32s.

Live imaging data analysis

Analysis was performed as described[17] and full code can be downloaded from https://www.dropbox.com/s/c8vn5uf5zsklgjj/mRNADynamics-

HernanDev.zip?dl=0. Histone-RFP slices were maximum projected for each time point. Nuclei were segmented using an object detection approach based on the Laplacian of Gaussian filter kernel. The segmented nuclei were then segmented and tracked over multiple nuclear cycles. Spots are detected in 3D and assigned to their respectively closest nucleus. When multiple spots are detected in the vicinity of a nucleus only the brightest one is kept. Spot intensity determination necessitates an estimate of the local fluorescent background for each particle. A 2D Gaussian fit to the peak plane of each particle column determines an offset, which is used as background estimator. The intensity is calculated by integrating the particle fluorescence over a circle with a radius of 6 pixels and then subtracting the estimated background. The imaging error is dominated by the error made in the fluorescent background estimation [17].

It is possible to measure the average fluorescence per polymerase molecule for the *hunchback enhancer >MS2* transgene with 24 MS2 repeats[17]. The quantitative imaging for the BAC transgenes were conducted under the exact same imaging conditions on the same microscope. The BAC transgenes also possess 24 MS2 repeats. However, the specific sequence of the stem loops are slightly different as these repeats have been further optimized to facilitate molecular biology work with them [30]. Assuming that the MS2 sites are similarly saturated in both cases we can then use the average fluorescence per polymerase molecule calculated for the *hunchback>MS2* transgene to calibrate the BAC fluorescent traces in terms of the absolute number of transcribing polymerases per fluorescent spot.

Mathematical Modeling

We propose a general scheme for enhancer promoter interactions which makes it possible to model the effect of having multiple enhancers activating a single promoter. Here the enhancer and promoter engage and disengage with one another, with some characteristic rate constants, k_{on} and k_{off}, respectively (See Fig. 4A). The ratio between k_{on} and k_{off} determine the strength of the promoter-enhancer interaction. While the enhancer is engaged with the promoter it is capable of producing mRNA at a rate r. We call this rate the transcriptional efficiency. By looking at the kinetics of transitions between different states it is possible to calculate the amount of mRNA produced at steady state, which is given by

$$mRNA = \frac{k_{on}}{k_{on} + k_{off}} * r$$

In Fig 4B we plot this rate as a function of the interaction strength for different values of the enhancer efficiency. Under a similar set of assumptions multiple enhancers would interact with a single promoter according to the scheme shown in Fig 4C. Again it is possible to calculate the amount of mRNA produced at steady state, which is given by the following equation:

$$mRNA = \frac{r^A k_{on}^A k_{off}^B + r^B k_{on}^B k_{off}^A}{k_{on}^B k_{off}^A + k_{on}^A k_{off}^B + k_{off}^A k_{off}^B}$$

By assuming the two enhancers have similar rates of interaction with the promoter one can simplify this expression to:

$$mRNA = \frac{k_{on}}{2k_{on} + k_{off}} * 2r$$

The plots of these different functions shown in Figure 4C illustrate how the amount of mRNA produced varies as a function the ratio (k_{on}/k_{off}).

Competing Interests

The authors declare no competing interests.

References

1. Jeong Y, El-Jaick K, Roessler E, Muenke M, Epstein DJ. A functional screen for sonic hedgehog regulatory elements across a 1 Mb interval identifies long-range ventral forebrain enhancers. *Development*. 2006;133(4):761–72. doi:10.1242/dev.02239.

2. Levine M, Cattoglio C, Tjian R. Looping Back to Leap Forward: Transcription Enters a New Era. *Cell*. 2014;157(1):13–25. doi:10.1016/j.cell.2014.02.009.

3. Perry MW, Boettiger AN, Levine M. Multiple enhancers ensure precision of gap gene-expression patterns in the Drosophila embryo. *Proc Natl Acad Sci U S A*. 2011;108(33):13570–13575. doi:10.1073/pnas.1109873108.

4. Frankel N, Davis GK, Vargas D, Wang S, Payre F, Stern DL. Phenotypic robustness conferred by apparently redundant transcriptional enhancers. *Nature*. 2010;466(7305):490–3. doi:10.1038/nature09158.

5. Lagha M, Bothma JP, Levine M. Mechanisms of transcriptional precision in animal development. *Trends Genet*. 2012;28(8):1–8. doi:10.1016/j.tig.2012.03.006.

6. Hong JW, Hendrix DA, Levine MS. Shadow enhancers as a source of evolutionary novelty. *Science*. 2008;321(5894):1314. Available at: http://www.mbi.osu.edu/2008/ws7materials/levine1.pdf.

7. Buecker C, Wysocka J. Enhancers as information integration hubs in development: lessons from genomics. *Trends Genet*. 2012:1–9. doi:10.1016/j.tig.2012.02.008.

8. Rada-Iglesias A, Bajpai R, Swigut T, Brugmann S a, Flynn R a, Wysocka J. A unique chromatin signature uncovers early developmental enhancers in humans. *Nature*. 2011;470(7333):279–83. doi:10.1038/nature09692.

9. Levine M. Transcriptional enhancers in animal development and evolution. *Curr Biol*. 2010;20(17):R754–63. doi:10.1016/j.cub.2010.06.070.

10. Nien C-Y, Liang H-L, Butcher S, et al. Temporal Coordination of Gene Networks by Zelda in the Early Drosophila Embryo. Barsh GS, ed. *PLoS Genet*. 2011;7(10):e1002339. doi:10.1371/journal.pgen.1002339.

11. Perry MW, Boettiger AN, Bothma JP, Levine M. Shadow enhancers foster robustness of Drosophila gastrulation. *Curr Biol*. 2010;20(17):1562–1567. doi:10.1016/j.cub.2010.07.043.

12. Miller SW, Rebeiz M, Atanasov JE, Posakony JW. Neural precursor-specific expression of multiple Drosophila genes is driven by dual enhancer modules with overlapping function. *Proc Natl Acad Sci U S A*. 2014. doi:10.1073/pnas.1415308111.

13. Arnold CD, Gerlach D, Stelzer C, Boryń ŁM, Rath M, Stark A. Genome-wide quantitative enhancer activity maps identified by STARR-seq. *Science*. 2013;339(6123):1074–7. doi:10.1126/science.1232542.

14. Lam DD, Souza FSJ De, Nasif S, et al. Partially Redundant Enhancers Cooperatively Maintain Mammalian Pomc Expression Above a Critical Functional Threshold. *PLoS Genet*. 2015:1–21. doi:10.1371/journal.pgen.1004935.

15. Gregor T, Garcia HG, Little SC. The embryo as a laboratory: quantifying transcription in Drosophila. *Trends Genet*. 2014;30(8):364–75. doi:10.1016/j.tig.2014.06.002.

16. Bothma JP, Garcia HG, Esposito E, Schlissel G, Gregor T, Levine M. Dynamic regulation of eve stripe 2 expression reveals transcriptional bursts in living Drosophila embryos. *Proc Natl Acad Sci U S A*. 2014;7:1–6. doi:10.1073/pnas.1410022111.

17. Garcia HG, Tikhonov M, Lin A, Gregor T. Quantitative imaging of transcription in living Drosophila embryos links polymerase activity to patterning. *Curr Biol*. 2013;23(21):2140–5. doi:10.1016/j.cub.2013.08.054.

18. Lucas T, Ferraro T, Roelens B, et al. Live imaging of bicoid-dependent transcription in Drosophila embryos. *Curr Biol*. 2013;23(21):2135–9. doi:10.1016/j.cub.2013.08.053.

19. Harrison MM, Li X-Y, Kaplan T, Botchan MR, Eisen MB. Zelda Binding in the Early Drosophila melanogaster Embryo Marks Regions Subsequently Activated at the Maternal-to-Zygotic Transition. Copenhaver GP, ed. *PLoS Genet*. 2011;7(10):e1002266. doi:10.1371/journal.pgen.1002266.

20. Perry MW, Bothma JP, Luu RD, Levine M. Precision of Hunchback Expression in the Drosophila Embryo. *Curr Biol*. 2012;22(23):2247–2252. doi:10.1016/j.cub.2012.09.051.

21. Gregor T, Wieschaus EF, Tank DW, Bialek W. Probing the limits to positional information. *Cell*. 2007;130(1):153–64. doi:10.1016/j.cell.2007.05.025.

540 22. Little SC, Tikhonov M, Gregor T. Precise developmental gene expression
541 arises from globally stochastic transcriptional activity. *Cell*.
542 2013;154(4):789–800. doi:10.1016/j.cell.2013.07.025.

543 23. Dunipace L, Ozdemir A, Stathopoulos A. Complex interactions between
544 cis-regulatory modules in native conformation are critical for Drosophila
545 snail expression. *Development*. 2011;4084:4075–4084.
546 doi:10.1242/dev.069146.

547 24. MacArthur S, Li X-Y, Li J, et al. Developmental roles of 21 Drosophila
548 transcription factors are determined by quantitative differences in binding to
549 an overlapping set of thousands of genomic regions. *Genome Biol*.
550 2009;10(7):R80. doi:10.1186/gb-2009-10-7-r80.

551 25. Kok K, Arnosti DN. Dynamic reprogramming of chromatin: paradigmatic
552 palimpsests and HES factors. *Front Genet*. 2015;6:29.
553 doi:10.3389/fgene.2015.00029.

554 26. Rushlow C, Shvartsman SY. Temporal dynamics, spatial range, and
555 transcriptional interpretation of the Dorsal morphogen gradient. *Curr Opin
556 Genet Dev*. 2012:1–5. doi:10.1016/j.gde.2012.08.005.

557 27. Venken KJT, Carlson JW, Schulze KL, et al. Versatile P[acman] BAC
558 libraries for transgenesis studies in Drosophila melanogaster. *Nat Methods*.
559 2009;6(6):431–4. doi:10.1038/nmeth.1331.

560 28. Di Talia S, Wieschaus EF. Short-term integration of Cdc25 dynamics
561 controls mitotic entry during Drosophila gastrulation. *Dev Cell*.
562 2012;22(4):763–74. doi:10.1016/j.devcel.2012.01.019.

563 29. Liu F, Morrison AH, Gregor T. Dynamic interpretation of maternal inputs by
564 the Drosophila segmentation gene network. *Proc Natl Acad Sci U S A*.
565 2013;110(17):6724–9. doi:10.1073/pnas.1220912110.

566 30. Hocine S, Raymond P, Zenklusen D, Chao JA, Singer RH. Single-molecule
567 analysis of gene expression using two-color RNA labeling in live yeast. *Nat
568 Methods*. 2013;10(2):119–21. doi:10.1038/nmeth.2305.

569

570

571

572

573

Figures

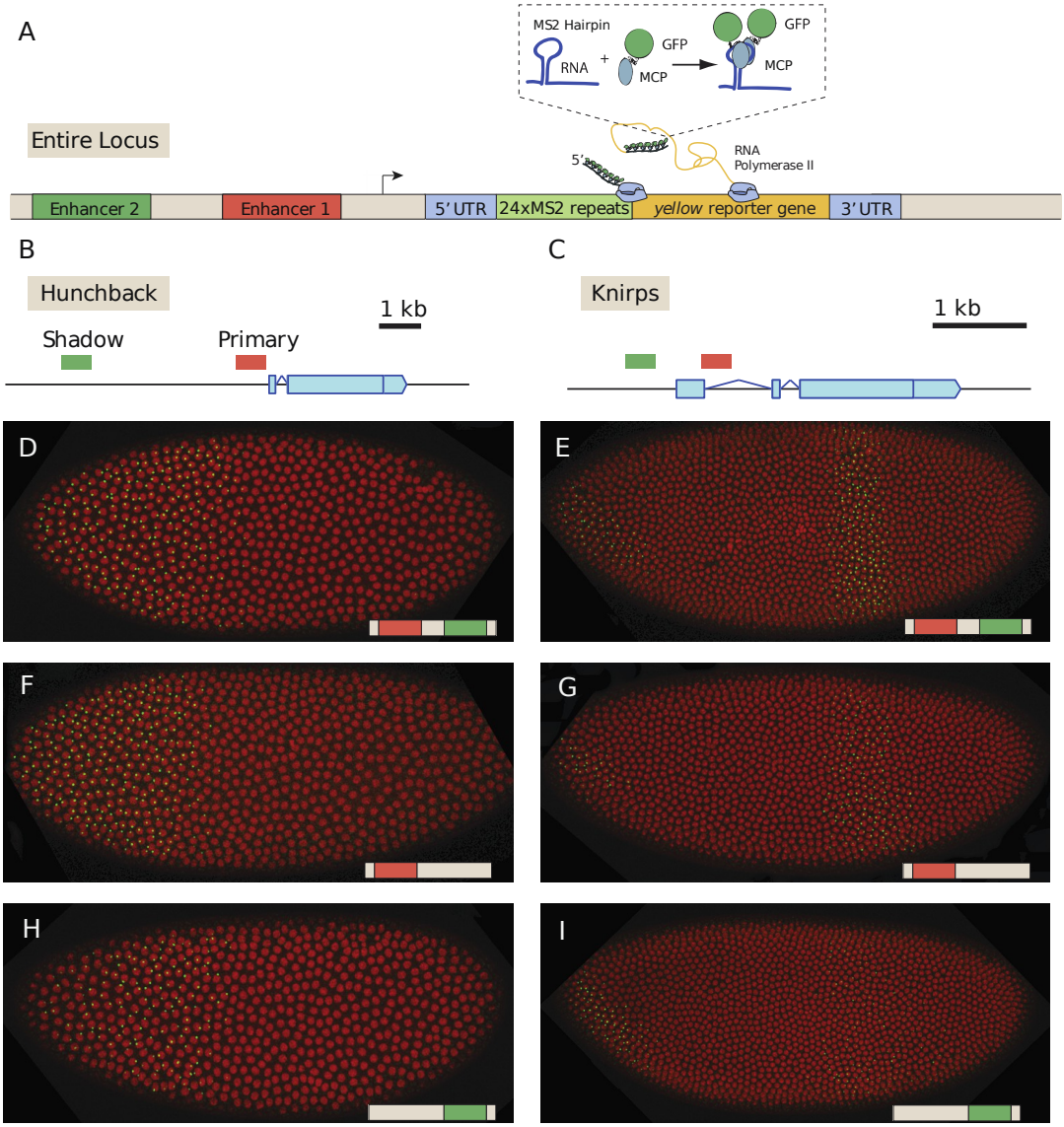

Figure 1: Live-imaging of transcriptional activity of *hb* and *kni* loci lacking different enhancers. (A) General structure of the reporter constructs. A reporter construct with 24 repeats of the MS2 stem loops and the *yellow* gene was recombined into BACs spanning the *hb* and *kni* loci. The 5' UTR and 3'UTR of the endogenous genes were left intact. The MCP::GFP protein that binds to the MS2 stem loops is present in the unfertilized egg and in the early embryo. Gene models of (B) the *hb* and (C) *kni* loci showing the location of the primary and shadow enhancers[3]. (D,F,H) Snapshots of *Drosophila* embryos expressing different versions of the *hb BAC*>MS2 reporter containing different combinations of the two enhancers 10 minutes into nuclear cleavage cycle 13 (nc13). The colored bar on the bottom right indicates which enhancer each line has removed. (E,G,I) Snapshots of a *Drosophila* embryos expressing different versions of the *kni BAC*>MS2 reporter containing different combinations of the two enhancers 10 minutes into nc13.

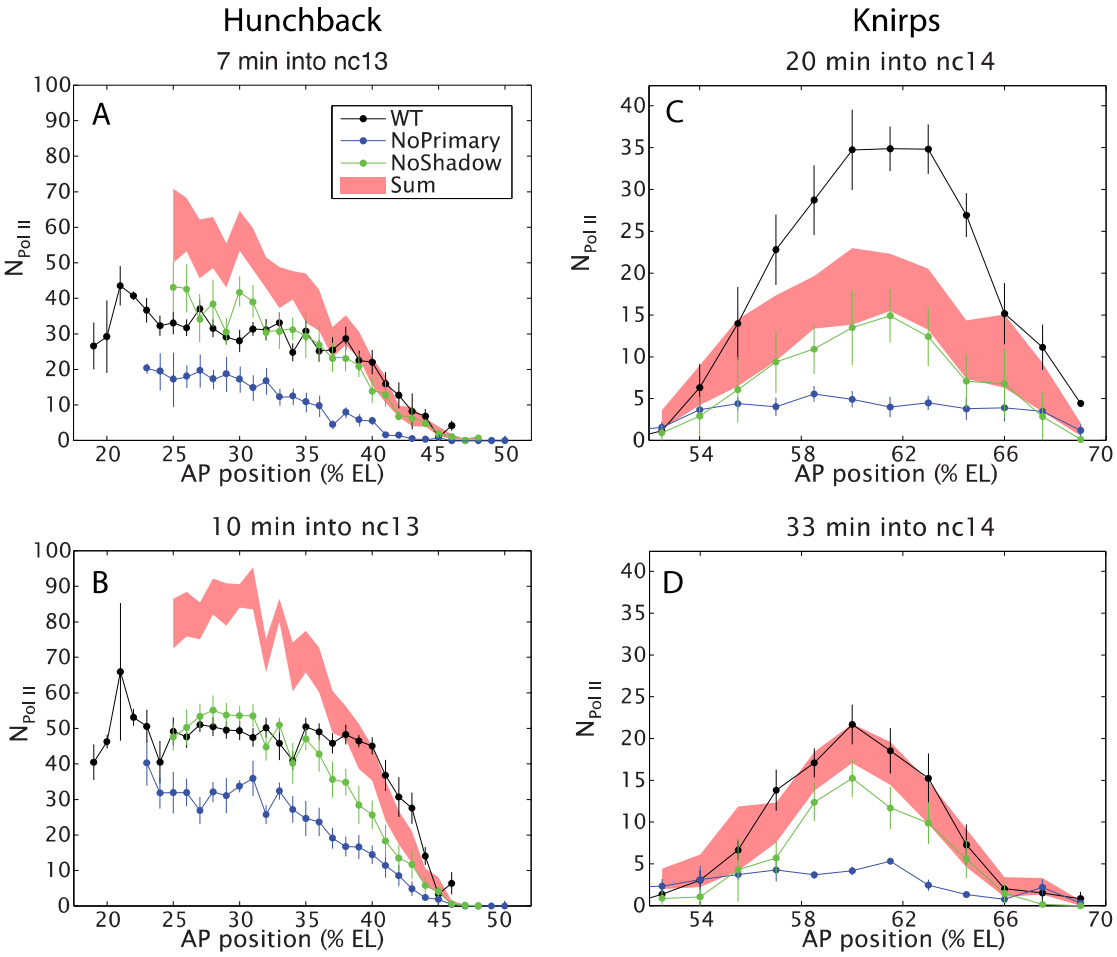

Figure 2: Combined effect of multiple enhancers as a function of AP position. (A,B) Mean number of Pol II molecules transcribing per nucleus ($N_{Pol\ II}$) in the *hb* BAC reporters containing different combinations of enhancers as a function of AP position for two time points in nc13. $N_{Pol\ II}$ is calculated by averaging data from at least three embryos at each AP position. The predicted sum of the individual enhancers is also shown. Note the additivity at the boundary versus the sub-additivity at the core, anterior domain of the pattern. (C,D) Mean number of Pol II molecules transcribing per nucleus ($N_{Pol\ II}$) in the *kni* BAC reporters in nc14 as a function of AP position (units relative to egg length, EL).. For *kni* we see super-additive behavior in the beginning of nc14 which then becomes additive later in nc14. The absolute number of transcribing Pol II molecules was estimated following a previous calibration[17]. Error bars are the standard error of the mean over multiple embryos.

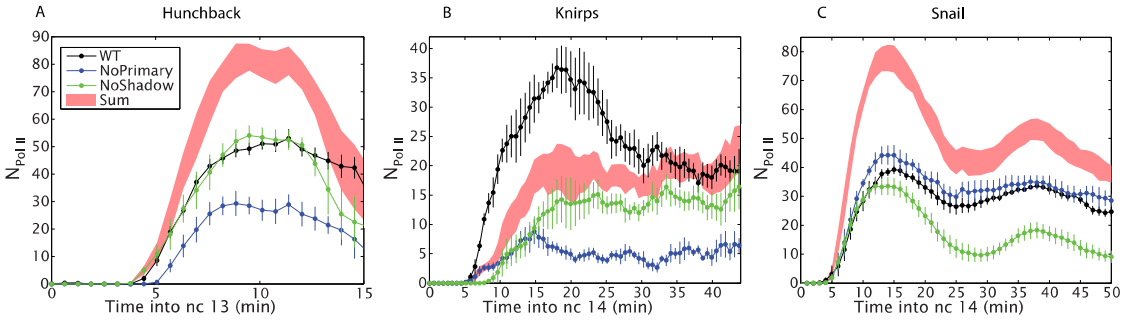

Figure 3: Combined effect of multiple enhancers as a function of time. (A) Time course of the mean number of Pol II molecules transcribing per nucleus ($N_{Pol\ II}$) for the different *hb* BAC transgenes and sum of individual enhancers at 27% EL for the duration of nc13. (B) *kni* BAC transgenes activities and the sum of individual enhancer activity at 60% EL for the first 50 min of nc14. (C) *sna* BAC transgenes and the sum of individual enhancer activities averaged over the central mesoderm for the initial 50 min of nc14. . Error bars are the standard error of the mean over multiple embryos.

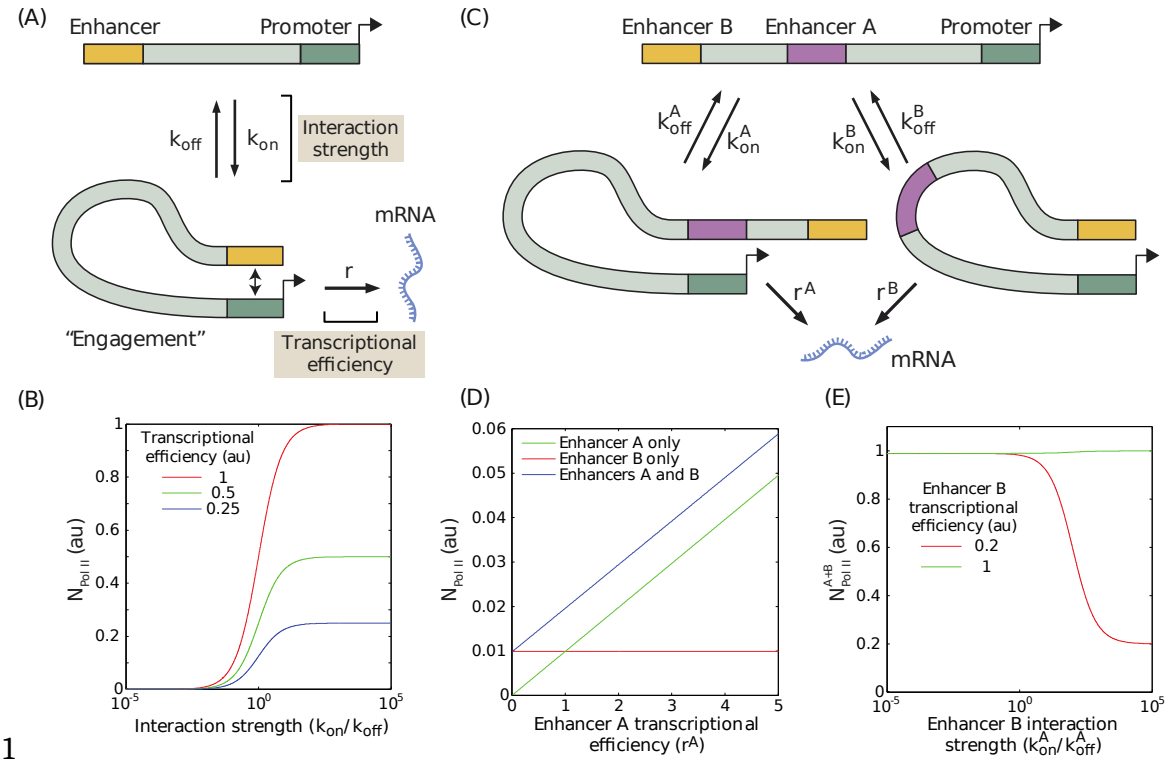

Figure 4. Model of enhancer promoter interactions and its predictions for mRNA production. (A) Minimal model of one enhancer engaging a promoter. k_{on} and k_{off} are the rates of promoter engagement and disengagement, respectively, and determine the interaction strength. r is the rate of mRNA production when the promoter is engaged and is a measure of the transcriptional efficiency. The mean number of Pol II molecules transcribing per nucleus ($N_{Pol\ II}$) is proportional to the rate of mRNA production. (B) As the interaction strength of a single enhancer is increased, the amount of mRNA produced increases up to a maximum value dictated by the transcriptional efficiency. (C) The model in (A) can be generalized to allow for multiple enhancers interacting with the same promoter. (D) In the regime where the interaction strength of both promoters is weak (k_{on}/k_{off}=0.01), the amount of mRNA produced by having both A and B is simply the sum of the individual contributions of A and B. (E) In the regime where the interaction strength is large, the combined activity of both enhancers can be significantly less than the sum the individual enhancers. A less efficient enhancer A (r^A=0.2 au) can interfere with the more efficient enhancer B (r^B=1 au) such that their combined activity is significantly less than the sum of the activities of individual enhancers.

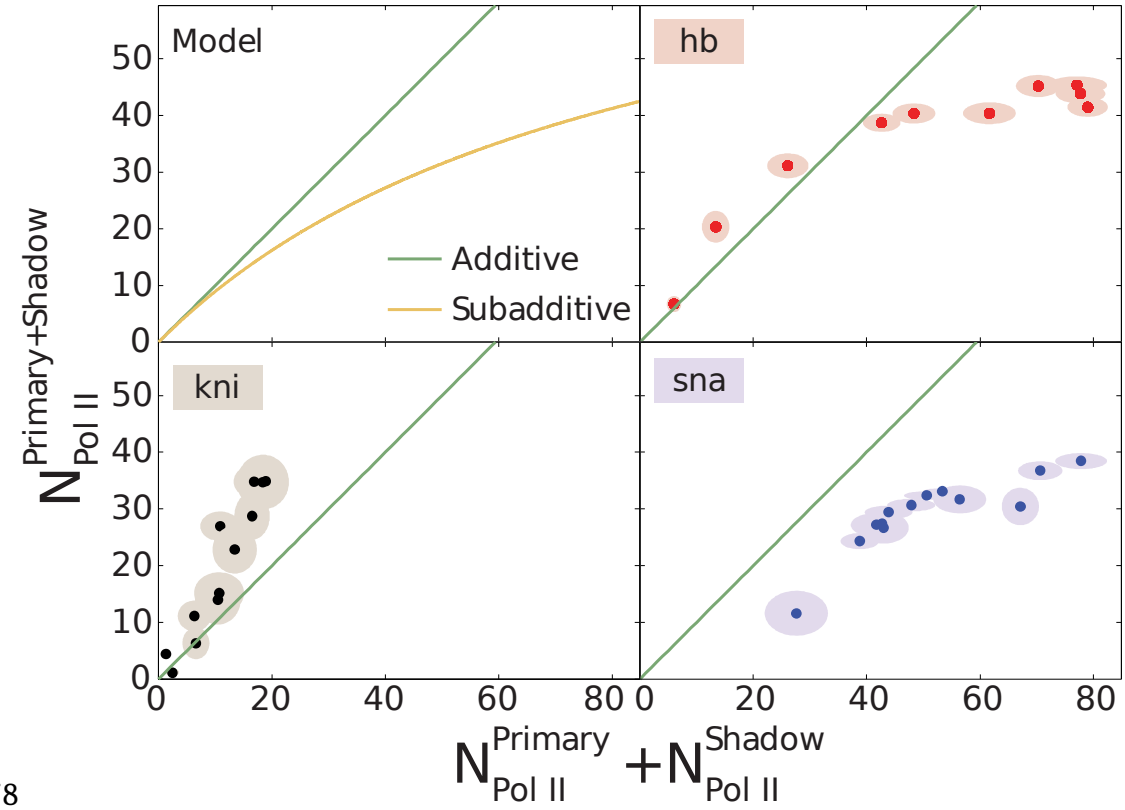

Figure 5: Different regimes of enhancer interaction. The yellow line shows the prediction for the rate of mRNA production from enhancers A and B varies with the sum of the individual rates of A and B as their interaction strength is varied. The green line shows perfect additivity. The model predicts additive behavior when the rate of production is low and subadditve behavior as the production rate increases. As the interaction strength of individual enhancers increases so does the rate of mRNA production, but the combined activity of both enhancers becomes subadditive. Transcriptional activity of intact loci (WT) versus the sum of activities of individual enhancers (NoShadow + NoPrimary) for *hb*, *kni* and *sna* at different times. A green line has been drawn in to indicate where WT is equal to NoShadow + NoPrimary. For *hb* and *kni* the plots show data taken at different AP positions at 10 min into nc 13 and 20 min into nc 14, respectively, while for *sna* the datapoints were at different times. Ellipses indicate standard error of the mean.

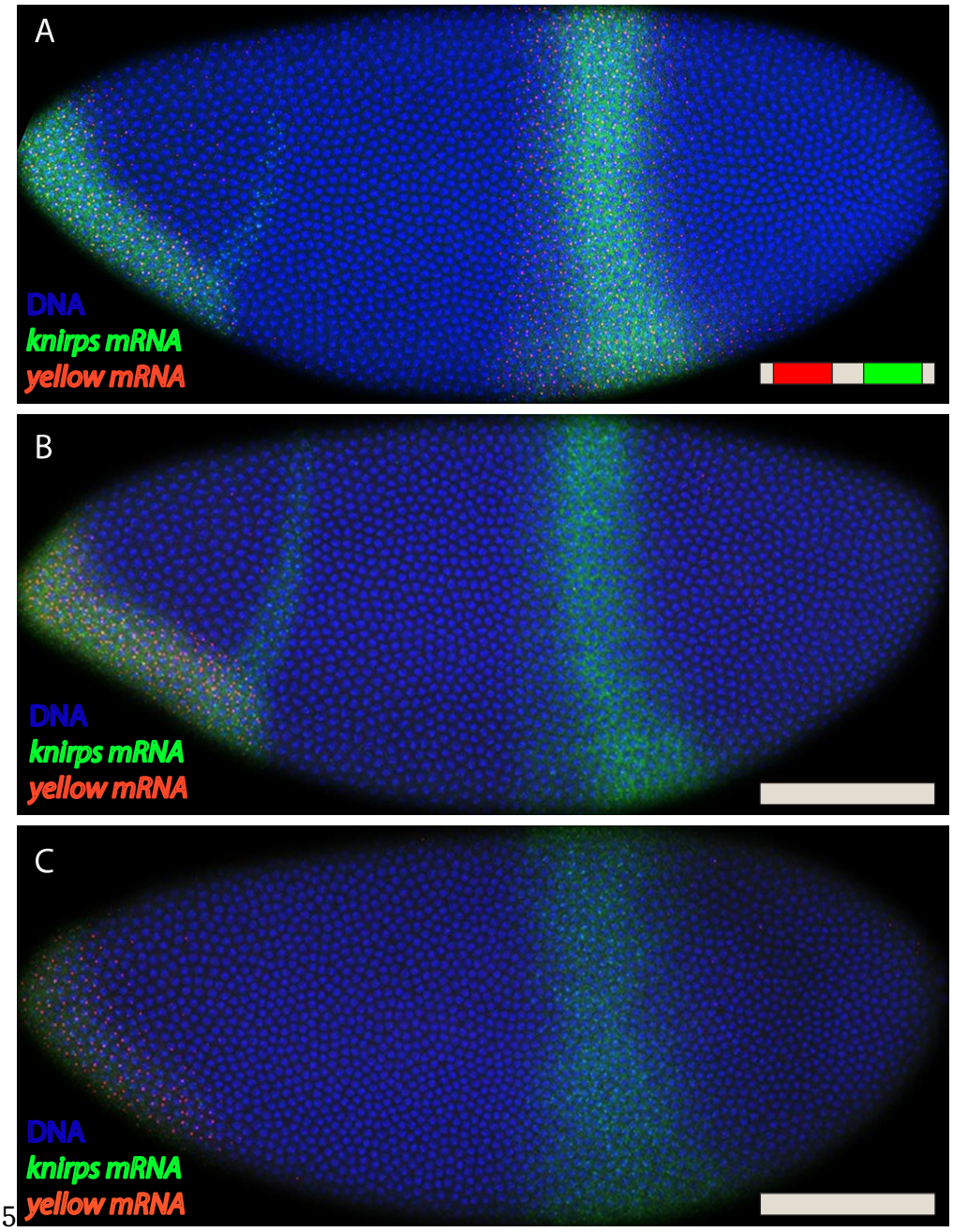

Figure S1: *kni* BAC expression lacking both shadow and primary enhancers. Fluorescent *in situ* hybridization of endogenous *kni* and *kni* BAC>yellow transgenes. (A) Shows an embryo with the fully intact kni BAC>yellow transgene in late nc 14. (B-C) Show embryos with the *kni* BAC>yellow transgene lacking both primary and shadow enahncers, Removing both enhancers abolishes all activity in the stripe domain. In (A) the an embryo is in late nc14 and (B) shows and embryo in early nc 14.

Movie 1: Dynamics of *hunchback* expression. Maximum projection of *hb* BAC>MS2 transgene from nc10 to gastrulation, MCP-GFP in green and histone in red, anterior to the left and ventral view up. Time elapsed since the start of imaging is indicated in top left. The initial pattern is restricted to the anterior where expression is driven by the primary and shadow enhancers. In late nc13 the central domain enhancer starts to be expressed.

Movie 2: Dynamics of *knirps* expression. Maximum projection of *kni* BAC>MS2 transgene from nc10 to gastrulation, MCP-GFP in green and histone in red, anterior to the left and ventral view down. Time elapsed since the start of imaging is indicated in top left. The dynamics of the anterior and central parts of the pattern are evident.

Movie 3: Dynamics of *snail* expression. Maximum projection of *snail* BAC>MS2 transgene from nc10 to gastrulation, MCP-GFP in green and histone in red, anterior to the left and ventral view up. Time elapsed since the start of imaging is indicated in top left.